

dat, Moscow, 1951.

<sup>9</sup>S. V. Vonsovskii, *Magnetizm (Magnetism)*, Nauka, 1971.

<sup>10</sup>R. Karplus and J. M. Luttinger, *Phys. Rev.* **95**, 1154 (1954).

<sup>11</sup>I. Kondo, *Prog. Theor. Phys.* **27**, 772 (1962).

<sup>12</sup>B. V. Egorov and M. A. Krivoglaz, *Fiz. Tverd. Tela (Leningrad)* **21**, 1416 (1979) [*Sov. Phys. Solid State* **21**, 817 (1979)].

<sup>13</sup>L. D. Landau and S. I. Pekar, *Zh. Eksp. Teor. Fiz.* **18**,

419 (1948).

<sup>14</sup>L. D. Landau and E. M. Lifshitz, *Kvantovaya mekhanika (Quantum Mechanics)*, Nauka, 1974 [Pergamon].

<sup>15</sup>M. A. Krivoglaz and G. F. Levenson, *Fiz. Tverd. Tela (Leningrad)* **9**, 457 (1967) [*Sov. Phys. Solid State* **9**, 349 (1967)].

Translated by J. G. Adashko

## Study of two-dimensional mixed state of type-I superconductors

I. L. Landau and A. E. Svistov

*Institute of Physics Problems, USSR Academy of Sciences*

(Submitted 23 October 1979)

*Zh. Eksp. Teor. Fiz.* **78**, 2287–2308 (June 1980)

We describe an experimental study of the destruction of superconductivity by current in hollow indium samples. In particular, we determine the destruction current  $I_{c2}$  of the two-dimensional mixed state and investigate the temperature dependence of the paramagnetic effect in a weak longitudinal magnetic field. In addition, we investigate the mixed state produced on the surface of a bulky cylindrical sample when a strong longitudinal magnetic field is abruptly turned off. Particular attention is paid to the study of the structure produced in a two-dimensional mixed-state layer in the presence of a weak transverse magnetic field. The velocity and the characteristic dimensions of the structure are measured at various values of the temperature and current density in the sample and of the transverse magnetic field.

PACS numbers: 74.30.Gn, 74.70.Gj

Destruction of the superconductivity of hollow type-I superconductors by current produces on their inner surface a thin layer of two-dimensional mixed (TM) state (private communication from L. D. Landau to D. Shoenberg, see Refs. 1 and 2). The TM state has been the subject of a number of experimental<sup>2-9</sup> and theoretical<sup>10-15</sup> studies. Nonetheless, many questions connected with the properties of the TM state remain unanswered to this day.

This paper consists of two methodologically different parts. In the first are described experimental study of the TM state produced on the inner surface of a hollow cylindrical sample. In particular, the current  $I_{c2}$  required to destroy the TM state has been measured. In addition to measurements of  $I_{c2}$ , we have investigated the temperature dependence of the paramagnetic effect of the TM state in a longitudinal magnetic field.

In the second part are described experimental studies of the TM state produced on the surface of a bulky cylindrical sample when an external magnetic field is turned off. This experiment, proposed by Dolgoplov and Dorozhkin,<sup>6</sup> is methodologically somewhat simpler than the destruction of the superconductivity of hollow cylinders by a current. On the other hand, the damping of the vortical currents produces in the TM-state layer nonstationary external conditions, thereby limiting somewhat the experimental possibilities. Particular attention was paid in the described experiments to the study of the structure produced in the TM state layer in a transverse magnetic field.

### 1. DESTRUCTION OF THE SUPERCONDUCTIVITY OF HOLLOW INDIUM CYLINDERS BY A CURRENT

#### Experimental setup

We used for the measurements two single-crystal samples<sup>1)</sup> with identical dimensions: outside diameter 8 mm, inside diameter 4 mm, and length 55 mm. The tetragonal axis was parallel to the sample axis. The resistance ratio  $R_{300\text{ K}}/R_0$  was 1700 and 1300 for samples 1 and 2 respectively. The currents through the samples (up to 1200 A) were produced by a current transformer with superconducting windings in accord with a previously described procedure.<sup>4</sup> The mounting of the samples is illustrated in Fig. 1. Two pairs of Helmholtz coils 4 and a solenoid 5, located in the immediate vicinity of the sample, could produce at the sample a magnetic field of any strength and direction.

The current needed to destroy the TM state was determined by measuring the surface impedance, using two coils  $L1$  and  $L2$ . The coils were flat spirals and had approximately 40 turns of copper wire of 20  $\mu\text{m}$  diameter each. The approximate dimensions of the coils and their arrangement in the sample cavity are shown in Fig. 1. The coils were connected in the tank circuit of a measuring rf oscillator, whose change of frequency was measured (and was proportional to the changes of the imaginary part of the surface impedance) as the state of the sample was varied. The oscillator frequency in these experiments was  $\sim 10$  MHz, and the change of frequency  $f_s - f_n$  when the sample went from

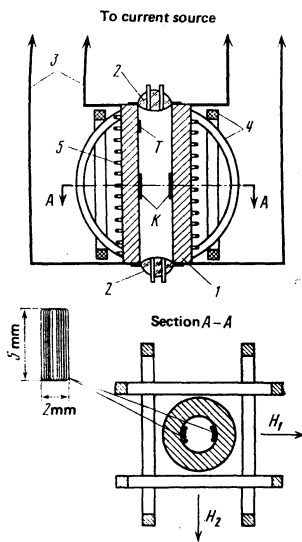


FIG. 1. Mounting the sample: 1—sample, 2—hermetic glass feed through insulators, 3—lead current conductors, 4—coils producing the transverse magnetic field, 5—solenoid;  $T$ —carbon thermometer,  $L$ —coil for the measurement of the surface impedance (an approximate picture of the coils is shown in the lower left).

the superconducting to the normal state was several dozen kilohertz. The oscillator frequency was measured with an electronic frequency meter Ch3-24 equipped with an analog readout.

The sample temperature was monitored in the course of the measurements with Allen-Bradley thermometers ( $T$  in Fig. 1), which were secured to the inner surfaces of the samples. Both openings of the sample were sealed and the leads from the thermometer and from the measurement coils were passed through hermetic glass feedthrough insulators. This procedure eliminated completely the errors due to the indeterminacy of the sample temperature even if the current raised the sample temperature much above that of the helium bath.

To measure the magnitude of the paramagnetic TM state in a longitudinal magnetic field we used an F-18 microwebermeter. The magnetic-field sensor was a coil of several thousand turns of copper wire of  $20 \mu\text{m}$  diameter. The coil was  $\sim 5 \text{ mm}$  long and placed in the central part of the sample cavity. The earth's magnetic field was compensated for accurate to  $\sim 0.02$ , using two pairs of Helmholtz coils located outside the cryostat.

#### Measurement of the impedance of the TM state at low currents

Figure 2 shows the dependence of the changes of the frequency of the measuring oscillator,  $\Delta f = f_s - f$ , on the

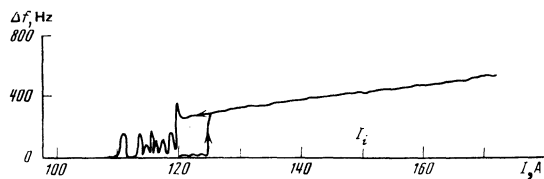


FIG. 2. Imaginary part of the surface impedance vs. current; sample 1,  $T = 2.9 \text{ K}$ ,  $f_s - f_n = 43 \text{ kHz}$ .

current in the sample. The abrupt increase of  $\Delta f$  when the current decreased to values below  $I_c$ , as well as the oscillations in time at  $I < I_c$ , is due to the motion of the residual parts of the normal phase of the sample, which no longer have axial symmetry, and their emergence to the outer surface of the sample. Similar phenomena were previously observed<sup>2</sup> in measurements with the aid of microcontacts.

The measurements of the surface impedance agree with the conclusion, previously drawn<sup>5</sup> from measurements of the current-voltage characteristics, that there is no intermediate state in samples of this geometry. In principle, an intermediate state can exist in hollow samples at currents only insignificantly higher than the critical value  $I_c = \frac{1}{2} c r_2 H_c$  ( $r_2$  is the outside radius of the sample). The superconducting regions can then emerge directly to the inner surface of the sample, and the normal states should be covered by a TM layer. The existence of the intermediate state becomes impossible if the current through the sample is

$$I > I_i = I_c \frac{r_1^2 + r_2^2}{2r_1 r_2}$$

( $r_1$  is the inside radius). Thus, at  $I > I_i$  the dependence of the surface impedance on the current characterizes the change of the properties of the TM-layer properties with changing current. At currents lower than  $I_i$ , however, if an intermediate state is produced in the sample volume, the surface impedance should decrease additionally on account of the appearance of superconducting regions that emerge to the outer surface of the sample and, as is well seen from Fig. 2, the character of the dependence of  $\Delta f$  on  $I$  remains the same up to  $I = I_c$ . That there is no intermediate state in such samples is also attested by the results, presented below, of measurements of the dependence of the paramagnetic effect on the current through the sample.

The absence of an intermediate state, which initially seemed quite strange, become quite understandable in light of the ideas reported in a preceding paper<sup>16</sup> concerning the intermediate state. In fact, for the investigated samples, the maximum possible diameter of the periodic structure of the intermediate state amounts at  $I = I_c$  to  $\sim 3 \text{ mm}$  (see Ref. 16), which is much less than the cavity diameter. Thus, only a Gorter structure of the intermediate state could exist in these samples.<sup>17, 18</sup> It should be noted that it does not follow at all from the described experiments that superconducting regions of the Gorter type are never produced in the interior of the sample. It can only be stated that the formation of such regions is so rare, that their contribution to the measured quantities is negligibly small.

#### Measurement of the TM-state destruction current

It turned out that the current at which the TM state is destroyed was tens of times larger than the critical value. At such currents account must be taken of a number of effects that can lead to substantial errors in the determination of  $I_{c2}$ . These effects include the overheating of the samples by the current and the appearance of a transverse magnetic field due to imperfections of the geometry of the sample and of the current lead. To

determine the value of this transverse field, we investigated the effect of an external transverse magnetic field on the impedance of the TM state at various currents in the sample. The results of these measurements are shown in Fig. 3.

If the external magnetic field is perpendicular to the surface of the sample in the region of the measuring coils, the dependence of the impedance on the field takes the form of a symmetrical curve with a minimum (Fig. 3a). The position of the minimum shifted in proportion to the current in the sample, with the positions of the minima on the  $\Delta f(H_1)$  curves being the same for both measuring coils. It is natural to assume that the position of the minimum corresponds to the instant when this magnetic-field component is cancelled out.

The dependence of the surface impedance on a field parallel to the sample surface is more complicated (Fig. 3b). Thus,  $\Delta f$  increases rapidly upon application of a magnetic field parallel to the magnetic field of the current in the TM-state layer, and varies more smoothly when the magnetic field is oppositely directed. From the symmetry of the curves plotted for different coils it is possible to determine in this case, too, the instant of cancellation of the transverse magnetic field.

After determining the dependences of both magnetic-field components on the current, it is possible to cancel out this field in the cavity of the sample and eliminate its influence on the properties of the TM state. To this end, both pairs of the coils that produced the transverse field were connected through corresponding voltage dividers to the same source used to supply the compensating coil of the current meter (see Ref. 4). The current through the coil then changed automatically in proportion to the current in the sample, and by suitable choice of the proportionality coefficient it was possible to maintain the transverse magnetic field in the cavity equal to zero for all changes of the current in the sample.

Figure 4 shows a plot of  $\Delta f$  against the current near  $I_{c2}$ . Simultaneously with plotting  $\Delta f$ , another  $x-y$  recorder was used to plot the resistance of the carbon thermometer ( $T$  in Fig. 1); such a plot is also shown in

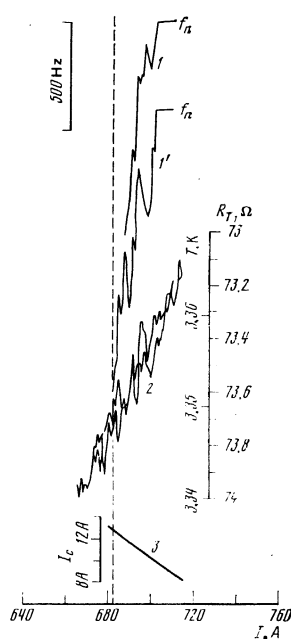


FIG. 4. Dependence of the parameters of sample 1 on the current near  $I_{c2}$ : 1 and 1'—successive plots of the surface impedance ( $f_s - f_n = 38$  kHz); 2—plots of carbon-thermometer resistance, 3—dependence of  $I_c$  on the current through the sample (recalculated from curve 2).

Fig. 4. The lower curve shows the change of  $I_c$  as a result of the overheating of the sample by the current. The strong oscillations on the plot of  $\Delta f$  against  $I$  are due to fluctuations of the sample temperature fluctuations produced when the helium boils intensely.

Figure 5 shows the ratio of  $I_{c2}/I_c$  as a function of the temperature for the two investigated samples. The values of  $I_{c2}$  determined with the two measuring coils agreed within the limits of the measurement accuracy. We also etched the inner surface of sample 2 with hydrochloric acid to remove a layer  $\sim 10^{-4}$  cm thick. This etching likewise failed to produce noticeable changes of  $I_{c2}$ .

The sharp decrease of  $I_{c2}/I_c$  when  $T_c$  is approached agrees with the theoretical calculations.<sup>10,11</sup> However, this agreement can not serve as a confirmation of one model or another, since this behavior of  $I_{c2}/I_c$  follows also from quite obvious considerations. In fact, the

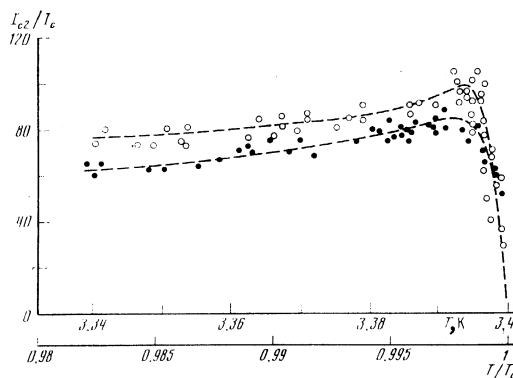


FIG. 5. Temperature dependence of  $I_{c2}/I_c$ : ●—sample 1, ○—sample 2.

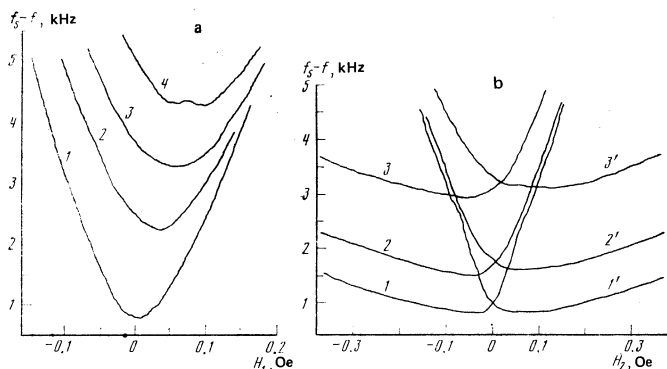


FIG. 3. Dependence of the impedance on the transverse magnetic fields: sample 1,  $T = 3.384$  K,  $I_c = 3.58$  A. a) Dependence on  $H_1$ : 1— $I = 4.5$  A; 2— $I = 15$  A; 3— $I = 25$  A; 4— $I = 35$  A. b) Dependence on  $H_2$ : 1, 1'— $I = 4.5$  A; 2, 2'— $I = 9$  A; 3, 3'— $I = 20$  A. The primes mark curves obtained with another measuring coil.

TM-state layer should be destroyed in any case if the current density  $j$  reaches a value such that  $jd_m \sim cH_0/4\pi$  ( $d_m$  is the smallest possible thickness of the TMstate). The layer thickness cannot be less than  $\xi(T)$ , and consequently increases as  $T_c$  is approached, and it is this which leads to a decrease of  $I_{c2}/I_c$  in proportion to  $1/\xi(T)$ . This greatly overestimates  $I_{c2}$ , inasmuch as a number of factors, such as the additional energy connected with the layer and others, make the destruction current much smaller.

Thus, the decrease of  $I_{c2}/I_c$  as  $T_c$  is approached is a more or less trivial fact if the thickness of the TM-state layer is of the order of  $\xi(T)$ . On the other hand, a decrease of  $I_{c2}/I_c$  with decreasing temperature and with increasing electric field (on going a sample with higher resistance) offer evidence that the processes that take place in the layer are of an essentially different character than assumed in the calculations.

### Temperature dependence of the paramagnetic effect of the TM state

If a sample with a TM-state layer on its inner surface is placed in a weak longitudinal magnetic field  $H_0$ , then the longitudinal magnetic field  $H_z$  in the cavity will greatly exceed the external field.<sup>4,9</sup> Such a paramagnetic effect was observed earlier in indium and tin sample, but the measurement interval was restricted to temperatures not too far from  $T_c$ . It was noted there that the magnitude of this effect is practically independent of temperature. In the present study we extended the measurement region to the entire temperature range attainable by pumping on He<sup>4</sup> vapor, and it turned out that the paramagnetic effect of the TMstate increased substantially when the temperature is lowered.

Figure 6 shows plots of the paramagnetic effect  $\mu$

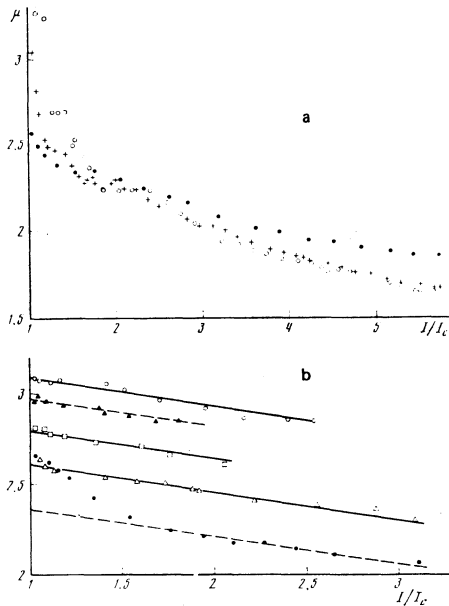


FIG. 6. Dependences of  $\mu = H_i/H_0$  on the current,  $H_0 = 0.05H_c$ , sample 1: a)  $\circ - T = 3.373$  K,  $I_c = 6.3$  A;  $+ - T = 3.361$  K,  $I_c = 9.3$  A;  $\bullet - T = 3.32$  K,  $I_c = 19.3$  A. b)  $\bullet - T = 3.32$  K,  $I_c = 19.3$  A;  $\Delta - T = 2.98$  K,  $I_c = 102$  A;  $\square - T = 2.62$  K,  $I_c = 182$  A;  $\blacktriangle - T = 2.13$  K,  $I_c = 250$  A;  $\circ - T = 1.34$  K,  $I_c = 400$  A.

$= H_i/H_0$  against the current through the sample, obtained at various temperatures. When the temperature is lowered,  $\mu$  increases noticeably; in addition, the form of the dependence of  $\mu$  on  $I$  also changes, particularly at currents close to critical.

It was initially assumed that the increase of  $\mu$  with decreasing current, which is observed at high temperatures, is due to the formation of an intermediate state in the interior of the sample. It turned out subsequently, however (see Refs. 5 and 16), that in samples of this geometry no intermediate state is produced even at  $I = I_c$ . The absence of an intermediate state is attested to also by the dependences of  $\mu$  on  $I$  at lower temperatures. In fact, if an intermediate state is produced in the vicinity of  $T_c$ , it should all the more be produced at lower temperatures, when the surface tension on the phase separation boundary decreases. Thus, the increase of  $\mu$  with decreasing current is due to the change of the properties of the TM state.

Figure 7 shows plots of  $\mu$  against  $T$  at various values of the current. The increase of  $\mu$  at  $I = 1.2I_c$  as  $T_c$  is approached is due to the change of the character of the dependence of  $\mu$  on  $I$ .

Bestgen<sup>12,15</sup> has considered the influence of the longitudinal magnetic field on a TM-state layer within the framework of the model of Andreev and Bestgen.<sup>11</sup> In this model, the TM state is a homogeneous layer in which the superconducting pairs are moved by an electric and a magnetic field. The theoretical calculations are valid in this case if the superconducting current  $I_s^*$  in the layer is small compared with the normal current  $I_n^*$  whereas the opposite is the case in the experiment ( $I_s^* \gg I_n^*$ ). It should be noted, however, that many theoretical conclusions are in quantitative agreement with the experimental results. This is all the more interesting since the paramagnetic sign of the effect was obtained under the assumption that the TM-state layer is perfectly homogeneous. On the other hand, it must be noted that the temperature dependence of the effect (Fig. 7) differs substantially from the theoretical predictions. Thus, according to Ref. 12, when the critical temperature is approached the paramagnetic effect should decrease in proportion to  $[\xi(T)]^{-3/4}$ , i.e., the paramagnetic effect should vanish near  $T_c$ , while in experiment the effect is observed also in the immediate vicinity of  $T_c$ .

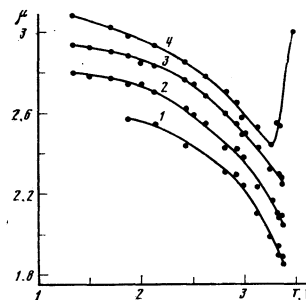


FIG. 7. Dependence of the paramagnetic effect on the temperature, sample 1,  $H_0 = 0.05H_c$ : curve 1— $I = 4I_c$ , 2— $I = 2.8I_c$ , 3— $I = 1.9I_c$ , 4— $I = 1.2I_c$ .

## 2. STUDY OF THE STRUCTURE OF THE TM STATE IN A TRANSVERSE MAGNETIC FIELD

### Experimental setup

The investigated sample was single-crystal indium in the form of a cylinder 8 mm in diameter and 150 mm long, with the tetragonal axis parallel to the crystal parallel to the sample axis. The resistance ratio (determined by measuring the damping of the vortical currents) was  $R_{300\text{ K}}/R_{0\text{ K}} = 3.2 \times 10^3$ . The sample mounting is illustrated in Fig. 8.

The longitudinal magnetic field (up to 700 Oe) was produced by a solenoid located outside the cryostat. For a more accurate orientation of the magnetic field parallel to the sample axis, two superconducting tin films were used (5 in Fig. 7). The resistance of the films in field much less than the critical value has a sharp minimum when the field is parallel to the film plane. The films were mounted perpendicular to each other on the same holder as the sample and were parallel to the sample axis with accuracy not worse than  $5'$ ; the accuracy of the parallelism of the magnetic field to the film planes was even several times higher. In addition, we were able to produce a weak (up to 60 kOe) transverse magnetic field using a pair of Helmholtz coils.

In these experiments we investigated the TM state produced on the sample surface after turning off the external magnetic field, and consequently as rapid a turning-off of the solenoid current was required. On the other hand, the solenoid that produced the longitudinal magnetic field was placed outside the cryostat, and had correspondingly larger geometric dimensions and a larger inductance, so that an abrupt turning-off of the current could damage the insulation of the solenoid. To limit the voltage of the solenoid, it was connected in parallel to several chains of KS630 avalanche diodes. When the circuit was opened the solenoid voltage was thus maintained constant at a level 800-

1000 V, and the field decreased linearly with time at a rate  $3.5 \times 10^4$  Oe/sec.

To study the structure produced in a TM-state layer in the presence of a transverse magnetic field, we used the microcontacts employed previously<sup>19, 20</sup> to investigate the dynamic intermediate state. The microcontacts were copper wires of 20  $\mu\text{m}$  diameter touching the sample surface. Up to five microcontacts were placed at the same time on the sample; the arrangement of the contacts for one of the experiments is shown in Fig. 8. To keep them from shifting, the microcontacts were glued to the sample after placement with highly diluted BF-2 adhesive.

To observe microcontact-resistance oscillations due to the motion of the normal domains in the TM-state layer we used an ac measurement setup. It consisted of two identical channels and could register simultaneously the resistance oscillations of any two microcontacts.

The block diagram of one of the channels is shown in Fig. 9. To increase the operating speed of the setup we used a measuring current of relatively high frequency (the operating frequency of one of the channels was 200 kHz, and that of the other 150 kHz). The alternating current flowed from the generator G through a resistance  $R_1 = 680$  and microcontact 2. The voltage from the microcontact was applied to the input of amplifier Amp; the amplified voltage was detected, smoothed by a chain of RC filters and fed to the input of one of the beam of the two-beam storage oscilloscope O. With the aid of the phase shifter PS and the variable resistor  $R_2$  it was possible to compensate for part of the voltage on the microcontact and by the same token increase the sensitivity of the setup. The transformers Tr1 and Tr2 decoupled the grounded circuits of the amplifier and generator.

The oscilloscope sweep was triggered by the delayed-pulse generator DPG, which was started at the instant when the magnetic field was turned off. Such a triggering method made it possible to investigate the pattern produced at various time intervals after turning off the magnetic field.

The operating speed of the measurement circuit is determined, in particular, by the bandwidth of the amplifier Amp. We have therefore constructed amplifiers

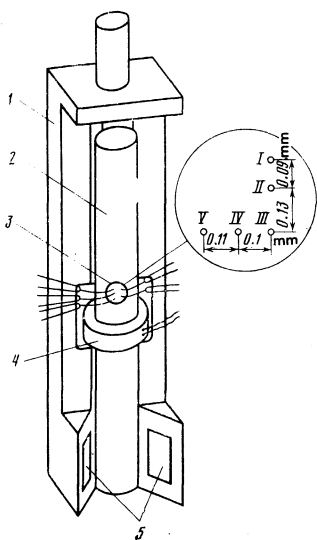


FIG. 8. Sample mounting: 1—holder, 2—sample, 3—microcontacts, 4—ballistic coil, 5—superconducting films for the adjustment of the magnetic field.

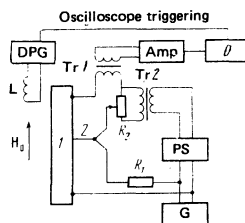


FIG. 9. Installation for the observation of the time variation of the microcontact resistance: 1—sample, 2—microcontact, G—GZ-33 sound generator, Amp—amplifier with full-wave rectifier at the output, PS—phase shifter, O—two-beam storage oscilloscope S1-51, DPG—delayed-pulse generator G5-35; Tr1 and Tr2—decoupling transformers, L—coil to trigger the DPG at the instant when the longitudinal magnetic field is turned off.

with bandwidths from 50 to 500 kHz; to exclude the mutual influence of the channels, resonant filters were connected in the amplifier, each tuned to the frequency of the other channel. The resultant operating speed was determined mainly by the time constant of the detector filter and amounted to  $\sim 20 \mu\text{sec}$  (the rise time of the rectangular pulse).

Simultaneously with the investigation of the layer structure with the aid of the microcontacts, we were also able to measure the rate of decrease of the longitudinal magnetic field in the sample by means of a ballistic coil (4 in Fig. 8) consisting of  $2 \times 10^4$  turns of  $20\text{-}\mu\text{m}$  copper wire.

### Measurement of the damping rate of the circular currents

After turning off the longitudinal magnetic field, whose value exceeds  $H_c$ , the magnetic field outside the sample is zero, and inside the sample it exceeds  $H_c$  as before; the situation on the sample surface is then perfectly analogous to the conditions on the inside surface of a hollow cylinder; this should lead to the onset of the TM state. The TM-state serve as it were as the connecting link between the region outside the sample, where the magnetic field is zero, and the normal metal in the central part of the sample, where the magnetic field is at any rate not less than the critical value.

The surface current density is close to  $cH_c/4\pi$  and depends little on the current density in the normal part of the sample.<sup>5,9</sup> The electric field in the TM-state layer is determined by the current density in the normal part in the sample and can be determined from the following simple considerations. In fact, if we neglect the thickness of the TM-state layer [which should be of the order of  $\xi(T)$ ] compared with the sample diameter, then it can be stated that the processes that take place in the sample (except for the layer occupied by the TM state) are fully analogous to the processes in a normal sample when the magnetic field is abruptly decreased to the value  $H_c$ .

Thus, if a TM-state layer is present on the sample surface, the magnetic field in the central part of the sample is only asymptotically close to the critical value, remaining at all time somewhat higher than  $H_c$ , and one might expect a situation wherein the normal state of the central part of the sample is maintained by currents in the TM-state layer, to last an arbitrarily long time. However, negligibly small inhomogeneities, which are always present in various samples, cause the TM-state layer to lose stability when the circular-current density is decreased, and the fluctuations of the layer thickness begin to increase. Individual sections of the layer are then converted into macroscopic superconducting regions that grow into the interior of the sample and crowd out the longitudinal magnetic field through the resultant normal regions. The axial symmetry is thereby upset.

The distribution the density of the circular currents in the sample assume after turning off the magnetic field the form

$$j(r, t) = -\frac{c(H_0 - H_c)}{2\pi r_0} \sum_{k=1}^{\infty} \frac{J_1(\mu_k r/r_0)}{J_1(\mu_k)} \exp\left(-\frac{t}{\tau_k}\right),$$

$$\tau_k = 4\pi\sigma r_0^2 / c^2 \mu_k^2,$$

where  $t$  is the time elapsed from the instant when the magnetic field is turned off,  $H_0$  is the turned-off magnetic field,  $\sigma$  is the conductivity of the sample in the normal state,  $r_0$  is the sample radius,  $J_1(x)$  is a Bessel function of first order, and  $\mu_k$  are the positive zeros of the Bessel function, numbered in increasing order.

The current density on the boundary of the TM-state layer with the normal part of the sample is  $j_n = j(r_0, t)$ . The voltage on the ballistic coil is

$$V = (2\pi r_0 / \sigma) j_n N, \quad (1)$$

where  $N$  is the number of turns in the coil.

Figure 10 shows in a semilog scale the time dependences of  $VH_0/(H_0 - H_c)$ . It is seen that the plots constructed in this manner coincide at high current densities with the curve (dashed) obtained for the sample in the normal state (at  $T > T_c$ ). At large values of  $t$ , meaning at low current density, the plots obtained at temperatures below  $T_c$  lie noticeably higher than the dashed curve on Fig. 10. This means that the rate of decrease of the longitudinal magnetic flux in the sample is higher than in a normal-metal sample under the same conditions. This increase in the rate of change of the magnetic flux is obviously due to development of instabilities in the TM-state layer and to the conversion of the latter into individual superconducting domains. All the measurements described below pertain the case of sufficiently high density of the circular current, when a TM-state layer exists on the sample surface and the function  $V(t)$  agrees with that calculated from Eq. (1).

The properties of the TM state should be determined by the current density in the sample normal part adjacent to the layer and by the intensity of the electric field in the TM-state layer. The average electric field in the layer coincides with the electric field in the normal metal near the layer, and the latter field is in turn proportional to the current density and to the resis-

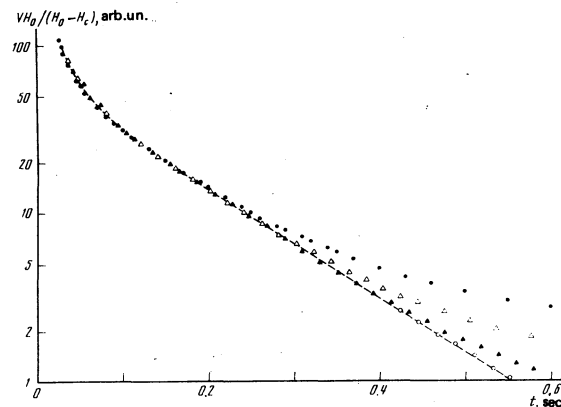


FIG. 10. Plots of  $VH_0/(H_0 - H_c)$  against the time elapsed from the instant when the longitudinal magnetic field was turned off:  $H_0 = 700$  Oe;  $\Delta$ — $T = 2.32$  K,  $H_c = 147$  Oe;  $\blacktriangle$ — $T = 2.96$  K,  $H_c = 65$  Oe;  $\circ$ — $T = 3.31$  K,  $H_c = 13$  Oe;  $\bullet$ — $T = 1.4$  K,  $H_c = 250$  Oe.

tivity of the normal metal. Thus, in this sample the properties of the TM state (at fixed values of the external magnetic fields) should be uniquely determined by specifying the density of the circular currents in the normal metal on the boundary with the TM-state layer,  $j_n$ , which can be naturally measured in units of  $\alpha = cH_0/4\pi r_0$ . Different values of  $j_n$  can be obtained either by measuring the delay time  $\tau_d$  between the instant when the magnetic field is turned off and the instant of observation. In most experiments  $H_0 = 700$  Oe, and  $j_n$  was varied by varying  $\tau_d$ .

#### Investigation of the TM-state structure with the aid of microcontacts

The dimensions of the contacts can be estimated from the change  $\Delta R$  of the resistance when the sample goes from the superconducting to the normal state.<sup>21</sup> The various investigated contacts had  $\Delta R$  in the interval  $6 \times 10^{-2} - 1.5 \times 10^{-3}$  ohms, corresponding to contact diameters from 0.3 to 1  $\mu\text{m}$ ; all the results reported below pertain to any contact.

Figure 11a show oscillograms (1, 2) of the voltage on the microcontact as a function of the time elapsed from the instant of magnetic-field turn-off, plotted at various measurement currents  $i$  through the contact. For small measurement contacts, the contact voltage rapidly reaches the value  $V_s$  corresponding to the superconducting state of the sample. With increasing  $i$ , the contact voltage exceeds  $V_s$  even when a noticeable time has elapsed after turning off the magnetic field. Thus, by the contact resistances we can differentiate between the superconducting and TM states. All the oscillograms of Fig. 11 were obtained at the same apparatus gain, and the voltage change  $V_n - V_s$  of the contact voltage on going from the superconducting state not only fails to increase in proportion to the current, but even decreases somewhat at larger measurement currents, i.e., the superconductivity in the region of the contact is partly destroyed at large measurement currents by the current flowing through the contact. This difference between the superconducting and TM state was observed also earlier<sup>2</sup> in dc measurements.

In our experiments, in the absence of a transverse magnetic field, no inner structure of the TM state was observed at all. However, in the absence of a magnetic field perpendicular to the sample surface in the region of the contacts, a structure was produced in the layer and moved under the influence of the current; this resulted in oscillations of the contact voltage (Fig. 11a, curve 3). The same situation is shown in greater detail in Fig. 11b. When a transverse magnetic field is applied, normal regions are produced in the layer, and the gaps between them are occupied as before by the TM state; this is attested by the fact that the minimum voltage on the contact remains noticeably higher than  $V_s$ .

The structure produced in the TM-state layer in a transverse magnetic field can be investigated by observing the motion of the regions between two contacts, in analogy with the earlier investigations of the dynamic intermediate state.<sup>19, 20</sup> Figure 12 shows oscillograms

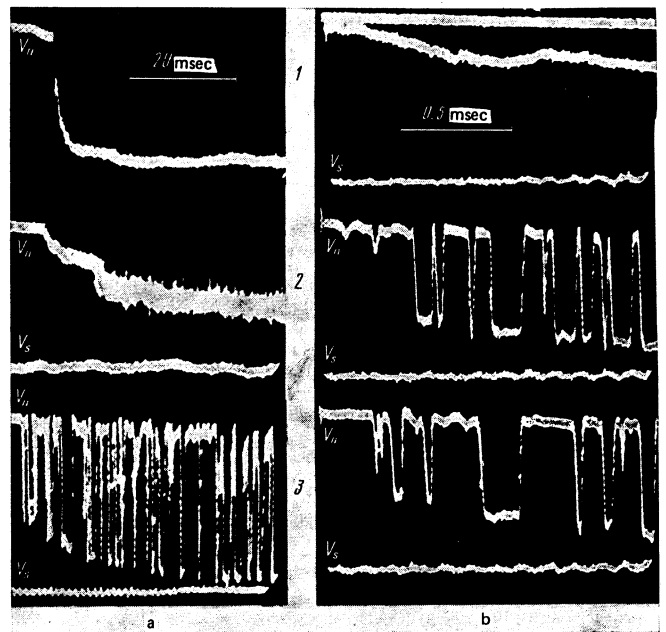


FIG. 11. Oscillograms of time dependence of microcontact voltage:  $T = 2.8$  K,  $H_c = 86$  Oe,  $H_0 = 725$  Oe. a)  $\tau_3 = 5$  msec: 1— $i = 0.7$  mA,  $H_1 = 0$ ; 2— $i = 9$  mA,  $H_1 = 0$ ; 3— $i = 9$  mA,  $H_1 = 7$  Oe. b)  $i = 6.5$  mA,  $\tau_d = 14.6$  msec: 1— $H_1 = 0$ , 2— $H_1 = 5$  Oe, 3— $H_1 = 9$  Oe.

of the voltages of two contacts. It is seen that all the irregularities of the voltage oscillations of one of the contacts are duplicated with some delay on the other, corresponding to a separation of 0.1 mm along the cylinder generator. The time shift is proportional in this case to the distance between the contacts (this was verified by measurements on different pairs of contacts). No correlations whatever were observed between the resistance oscillations of contacts placed in the intersection of the cylinder with a plane perpendicular to its axis (for example, contacts III, IV, and V in Fig. 8). It can be concluded on this basis that the structure in the layer moves in a direction perpendicular to the current in the sample. This structure, at least at small values of  $H_1$ , should take the form of closed normal-phase regions surrounded by a layer of the TM state.

By measuring the time of motion of the structure between the contacts, we can determine the speed  $v$  and the period  $a$  of the structure. Figure 13 shows the dependences of the average period of the structure on the

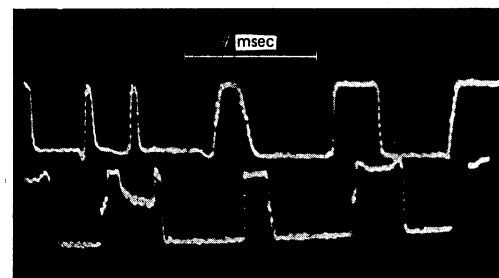


FIG. 12. Oscillogram of voltage on two microcontacts. Distance between contacts 0.1 mm.  $T = 2.8$  K,  $H_c = 86$  Oe,  $H_0 = 725$  Oe,  $H_1 = 19$  Oe,  $\tau_d = 100$ .

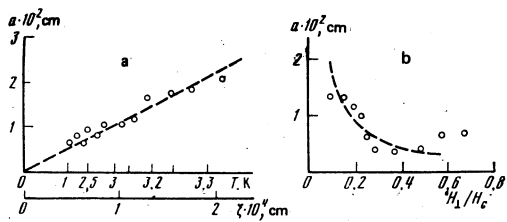


FIG. 13. Dependence of the average period of the structure on the temperature and on the transverse magnetic field: a)  $a(T)$  at  $H_1 = 0.18H_c$ , b)  $a(H_1)$  at  $T = 3.06$  K;  $H_c = 52$  Oe,  $H_0 = 700$  Oe,  $j_n = 6.9\alpha$  ( $\alpha = cH_c/4\pi r_0$ ). Here and in the captions of the figures that follow we indicate the quantity  $j$  corresponding to the given delay time with the transverse magnetic field turned off. The dashed line is a plot of  $a \propto 1/H_1$ .

temperature and on the transverse magnetic field  $H_1$ . The results obtained at the same values of  $H_1/H_c$  and  $j_n/\alpha$  were compared at different temperatures. At small  $H_1$  the period of the structure varied with temperature approximately in proportion to the coherence length (Fig. 13a); with decreasing  $H_1$ , the period increased approximately in proportion to  $1/H_1$ . In Fig. 13,  $\xi$  is a parameter that characterizes the surface tension on the phase separation boundary;<sup>22</sup> this tension in indium differs from  $\xi$  by a numerical factor close to unity.

The speed of the structure  $v$  increased with increasing  $j_n$  and with decreasing  $H_1$ . Figure 14 shows plots of  $j_n/v\alpha$  against  $H_1$  at various temperatures and various values of  $j_n$ . At low temperatures and small  $j_n$ , the speed is approximately proportional to  $1/H_1$ . With increasing  $j_n$  and with rising temperature the proportionality region practically vanishes. The solid curves in Fig. 14a pass through the experimental points symmetrically relative to the origin, and illustrate the fact that the change of the sign of  $H_1$  corresponds to a reversal of the direction of motion. The direction of the motion was reversed also when the direction of  $j_n$  was reversed (this corresponds to a reversal of the sign of the turned-off magnetic field  $H_0$ ).

Figure 15 shows the temperature dependences of the speed at various values of  $H_1$ , with the ordinates repre-

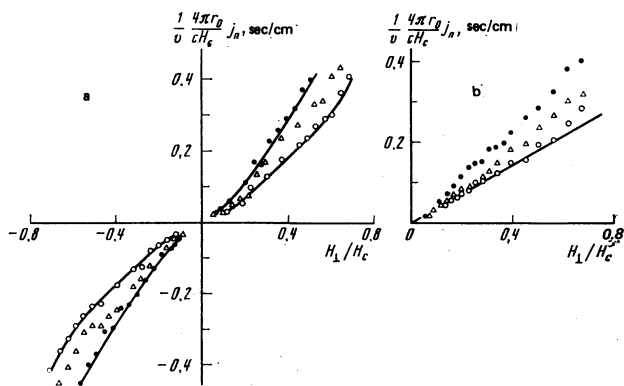


FIG. 14. Plots of  $j_n/v\alpha$  against the transverse magnetic field:  $H_0 = 700$  Oe. a)  $T = 3.24$  K,  $H_c = 24.6$  Oe:  $\bullet$ — $\tau_d = 200$  msec,  $j_n = 13.8\alpha$ ;  $\Delta$ — $\tau_d = 290$  msec,  $j_n = 6.9\alpha$ ;  $\circ$ — $\tau_d = 384$  msec,  $j_n = 3.5\alpha$ . b)  $T = 2.81$  K,  $H_c = 84$  Oe:  $\bullet$ — $\tau_d = 57$  msec,  $j_n = 13.8\alpha$ ;  $\Delta$ — $\tau_d = 116$  msec,  $j_n = 6.9\alpha$ ;  $\circ$ — $\tau_d = 205$  msec,  $j_n = 3.5\alpha$ .

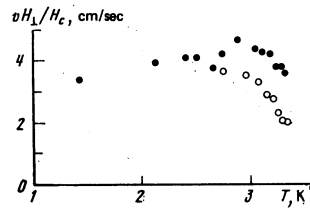


FIG. 15. Plot of  $vH_1/H_c$  vs. temperature:  $\bullet$ — $H_1 = 0.18H_c$ ,  $\circ$ — $H_1 = 0.36H_c$ .

sents the quantity  $vH_1/H_c$ . The discrepancy between the curves at increased temperatures indicates deviations from the  $v \propto 1/H_1$  law.

We measured also in these experiments the concentration  $C_n$  of the normal phase on the sample surface by connecting an integrating RC network between the detecting amplifier and the oscilloscope (see Fig. 9). The time constant of this network was chosen such that  $C_n = (V - V_s)/(V_n - V_s)$ , where  $V_n$  is the voltage on the contact when the entire sample is normal,  $V_s$  is the voltage on the contact when the entire sample is superconducting, and  $V$  is the voltage on the contact in the presence of a moving structure. The measurements of  $C_n$  were made with weak currents at which the TM state (relative to the voltage on the contact) was indistinguishable from the superconducting state. The measured  $C_n(H_1)$  dependences are shown in Fig. 16. The solid lines are drawn so that their slopes are the same in the right and left parts of the diagram are equal. Some asymmetry of the results is due to inaccuracy in the orientation of the longitudinal magnetic field  $H_0$ , which leads to the appearance of a transverse magnetic field proportional to  $H_0$  and to the angle between  $H_0$  and the sample axis.

The average magnetic field in the normal regions near the sample surface is  $H_1 = H_1/H_c$  (we have assumed that all the transverse magnetic field is concentrated in the normal regions).  $H_1$  is noticeably weaker than  $H_c$  at large  $j_n$ .

A small rotation of  $H_1$  in a plane perpendicular to the sample axis did not lead to a noticeable change in the results. Rotation of  $H_1$  through an angle  $90^\circ$  from the direction perpendicular to the sample surface in the region of the contacts caused the structure to vanish.

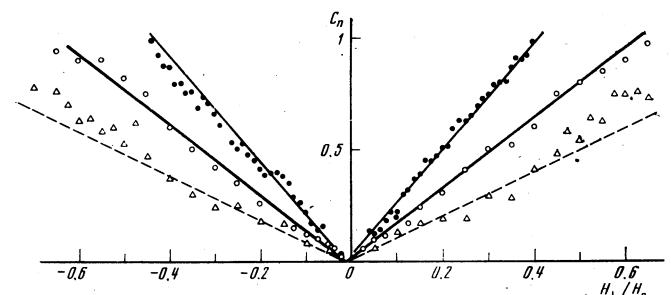


FIG. 16. Dependences of the concentration of the normal phase on the sample surface on the transverse magnetic field;  $T = 3.14$  K,  $H_c = 40$  Oe,  $H_0 = 700$  Oe:  $\bullet$ — $\tau_d = 35$  msec,  $j_n = 56\alpha$ ;  $\circ$ — $\tau_d = 268$  msec,  $j_n = 5.1\alpha$ ;  $\Delta$ — $\tau_d = 800$  msec,  $j_n = 0.09\alpha$ . The dashed lines correspond to the relation  $C_n = H_1/H_c$ .

### 3. DISCUSSION OF RESULTS

We were unable to observe in the described experiment any regular internal structure in the TM-state layer without a transverse magnetic field. We shall therefore discuss the results assuming that the TM-state is practically homogeneous. Such a layer differs from a thin superconducting layer, generally speaking, only in that it contains an electric field that coincides, in the absence of a transverse magnetic field, with the electric field in the normal metal.

The presence of a transverse magnetic field leads in this case to a destruction of the TM-state layer and to formation of a peculiar intermediate state in which the role of the superconducting regions is played by regions occupied by the TM state. It must be borne in mind here that the appearance of normal region in the TM state layer causes part of the electric field to be concentrated in the normal regions and the electric field to increase accordingly in the regions of the TM state. This assumption is confirmed by the oscillograms shown in Fig. 11. One might expect a sufficiently strong magnetic field to cause the entire electric field to be concentrated in the normal regions and the TM state to become superconducting, but this is possible only if the period of the structure is small compared with the layer thickness. Actually, however, the period of the structure (see Fig. 13) is not small, and the thickness of the TM-state layer should be of the order of  $\xi(T)$ . The fact that the dimensions of the normal domains exceed  $\xi(T)$  appreciably in this case is not surprising, since measurements of superconducting films show that in the case when the normal domains constitute closed regions, and the film thickness is of the order of the coherence length, the size of the normal domains exceeds appreciably the film thickness.<sup>23</sup>

It must be emphasized that even the fact that the characteristic dimensions of the structure (produced in the presence of a transverse magnetic field) turned out to be large compared with the layer thickness is evidence of the presence of an electric field in the regions occupied by the TM state. Actually, all of the arguments advanced concerning the necessity of the existence of a layer of the TM state (in which superconductivity and an electric field coexist) can be repeated also with respect to an individual TM-state region, on the sample surface, with dimensions along the surface large compared with its thickness.

The period of the structure of the intermediate state is determined usually by a relation of the type  $a = \text{const} \times (d\xi)^{1/2}$ , where  $d$  is the characteristic dimension of the region occupied by the intermediate state. The proportionality of the period to  $\xi(T)$  is thus evidence that in this case the layer thickness  $d \sim \xi(T)$ .

Andreev<sup>24</sup> considered theoretically the destruction of the superconductivity of a plane-parallel plate by a current. He has shown that in the absence of a transverse magnetic field the problem has no solution in the form of an intermediate state. It is known now that a TM state is produced in this case. In the presence of a transverse magnetic field the equations of the macro-

scopic electrodynamics of the intermediate state already have a solution. This solution can be applied to our case, but this requires satisfaction of the inequality  $\xi(T) \ll a \ll d$  ( $a$  is the period of the structure). In the case of a cylindrical sample it is necessary also to stipulate  $d \ll r_0$ .

Actually the period of the structure has turned out to be not at all small; therefore the case considered by Andreev<sup>24</sup> could be realized only at very small  $j_n$  (the layer thickness increases with decreasing  $j_n$  and at sufficiently small  $j_n$  the inequality  $a \ll d$  should apparently be satisfied). At small  $j_n$  however instabilities arise in the TM-state layer and lead to loss of axial symmetry. We emphasize that the development of an instability of this type is due to the fact that in this experiment a given total magnetic flux in the sample was used. Under other conditions, for example in a plate, when the value of the current is specified, the situation considered in Ref. 24 can be realized.

To determine the speed of the structure in the TM-state layer it is possible, in principle, to use equations similar to those obtained by Andreev and Sharvin<sup>25</sup> for the description of the dynamic intermediate state. These equations were obtained from the condition of continuity of the tangential component of the electric field on the phase-separation boundary, and the velocity in the direction perpendicular to the electric and magnetic fields can be expressed in the form

$$v = c(E_1 - E_{TM})/H_1, \quad (2)$$

where  $H_1$  is the magnetic field in the normal region near the boundary with the TM-state layer, and  $E_1 - E_{TM}$  is the difference between the electric fields in the normal region and in the TM-state layer. It is, however, a very complicated matter to use Eq. (2) for the description of the real situation in the TM-state layer. The point is that this equation gives the velocity in a direction perpendicular to the magnetic field. Outside the sample the magnetic field is perpendicular to the surface, and in the normal part of the sample near the boundary with the layer the field makes an angle of the order of  $[H_1(H_c^2 - H_1^2)^{-1/2}]$  with the sample surface. In the case of a thin TM-state layer it can apparently be assumed that the magnetic field in the normal region is inclined by a certain average angle, which in the case  $H_1 \ll H_c$  is of the order of  $H_1/H_c$ . In this case the velocity measured on the surface of the sample will be  $H_c/H_1$  times larger than the real velocity of the interphase boundaries. This possibly is in fact the cause of the increased velocity with decreasing  $H_1$ .

Another circumstance that hinders a comparison of the results with Eq. (2) is the uncertainty in the value of  $E_1 - E_{TM}$ . Application of a transverse magnetic field leads to an increase of  $j_n$  (since the current in the TM-state layer decreases) and of the average value of the circular electric field. Since the period of the structure turned out not to be small, it is very difficult to estimate theoretically  $E_1 - E_{TM}$  for this case. Experiment (measurement of the voltage across the ballistic coil) can determine only the increase of the electric field averaged over the perimeter of the sample. In this case it is necessary to recognize that the growth

of the electric field will vary with the angle between the external magnetic field and the normal to the sample surface. Thus, even though (2) can formally be used to determine the speed of the structure in the TM-state layer, it is hardly possible to determine the characteristics of the TM state by comparing this equation with the experimental results.

Another interesting circumstance is the noticeable broadening of the oscillograms obtained at large measuring currents (Fig. 11a). The point is that with increasing measuring current the resolving power of the microcontact can only deteriorate; thus, this broadening can not be a manifestation of some TM-state "microstructure" that is unresolvable at weaker measurement currents. This effect is possibly due to the fact that a strong measurement current can lead to destruction of the outer part of the TM layer, and makes the microcontact "more sensitive" to nonstationary processes that take place near the boundary between the layer and the normal part of the sample.

The results reported in this part of the article are in good agreement with the data obtained by Dolgoplov and Dorozhkin<sup>6,7</sup> in a study of the TM state produced under similar conditions on the surface of a rectangular aluminum sample. To be sure, it must be noted that in our experiments we observed no normal regions elongated in the magnetic-field direction and moving along the current. Such regions were observed in Refs. 6 and 7 when a relatively weak magnetic field was turned off, corresponding to a low current density in the normal part of the sample. It is possible that the formation of such region is due to instabilities in the TM-state layer and was not observed in our experiments, since we performed no measurements with weak currents. On the other hand, the superconducting properties of aluminum differ greatly from those of indium, and the existence of such regions may be due to the relatively large surface tension on the boundary between the different phases in aluminum.

## CONCLUSION

While a number of theoretical papers on the TM state have been published in the last few years, it must nevertheless be stated that the theoretical premises concerning the structure of the TM state apparently still do not describe the real situation. Thus, the experiments described in this article contradict to some degree or another all the theoretical modes of the layer.

We note first that the investigation of the TM state with the aid of microcontacts indicates that this state, at any rate, does not have a regular periodic structure similar to the intermediate state. Indeed, if such a structure were to exist and were for some reason unresolvable with the aid of microcontacts, it should manifest itself in the presence of a transverse magnetic field by breaking up into separate superconducting and normal domains. The normal domains should increase in this case gradually with increasing transverse magnetic field. On the other hand, investigations of the structure produced in a transverse magnetic field

have shown that at the lowest values of the transverse magnetic field macroscopic normal regions appear in the layer, and neither in our experiments with indium nor in Dolgoplov's and Dorozhkin's experiments with aluminum did the normal regions decrease noticeably in size with decreasing transverse magnetic field.<sup>2)</sup> These experiments thus disagree quite strongly with the theoretical models of the periodic structure of the TM-state layer structure.<sup>13,14</sup> We note also that these two models predict a very rapid change of all the layer parameters with decreasing current near the critical value (this pertains to hollow cylindrical samples), whereas our measurements of the impedance of the TM state (Fig. 2) as well as the previously reported measurements of the current voltage characteristics,<sup>5</sup> differ from these theoretical predictions.

As for presently proposed models of the homogeneous TM-state layer,<sup>10,11</sup> they cannot be compared with the experiments, since the region of their validity is quite far from the real experimental situation. Thus, the model developed by Andreev and Tekel<sup>10</sup> is valid for the case when the electric field in the sample  $E \equiv 0$ , and describes in fact simply a thin superconducting layer. The model developed by Andreev and Bestgen,<sup>11</sup> on the other hand, pertains to the opposite limiting case when the superconductivity in the TM-state layer is destroyed to such an extent that the small number of superconducting pairs in the layer can be regarded as fluctuations.

It is of interest to note, nevertheless, that Bestgen<sup>12,13</sup> considered the influence of a longitudinal magnetic field on a TM-state layer within the framework of the model proposed in Ref. 11, and showed that many theoretical conclusions agree qualitatively with the experiments. This includes the correct sign of the effect when the TM-state layer is on the outer or inner surface of the sample, the absence of the effect when this layer is in the interior of the sample, as well as the instabilities observed at large values of the longitudinal magnetic field (see Refs. 4 and 9) and the decrease of the paramagnetic effect with rising temperature (see Fig. 7). This agreement is of particular interest also because formally the theoretical calculations do not hold for our experimental situation.

On the other hand, it is difficult to imagine that the above-noted qualitative agreement between theory and experiment in various aspects of the behavior of the TM-state layer in a longitudinal magnetic field is simply fortuitous. It seems to indicate that this behavior of the superconducting condensate in the presence of parallel electric and magnetic fields is actually a more general circumstance and is preserved at any ratio of  $I_s^*$  and  $I_n^*$  ( $I_s^*$  and  $I_n^*$  are respectively the superconducting and normal currents in the TM-state layer).

The structure of the TM state is of great interest, since it constitutes some new type of resistive state of superconductors. It appears that an important role is played in the TM-state layer by kinetic and nonstationary processes connected with the coexistence of superconductivity and an electric field.

In conclusion, we consider it our pleasant duty to

thank Yu. V. Sharvin for constant interest in the work much helpful advice, A. F. Andreev, V. T. Dolgoplov, and S. I. Dorozhkin for a discussion of the questions touched upon here, and V. I. Voronin for help with the design of the electronic circuitry.

#### SUPPLEMENT (11 MARCH 1980)

Dorozhkin and Dolgoplov describe in a recent detailed paper<sup>26</sup> further experimental study of the TM state produced on the surface of a rectangular aluminum sample following the turning-off of a longitudinal magnetic field. The essential difference between their results and ours is the observation of normal regions in the TM-state layer even in the case when the turned-off magnetic field is parallel to the sample surface. We would like therefore to discuss this question further.

One of the possible causes of such a structure could be a transverse magnetic field produced when the currents become redistributed after the external magnetic field is turned off. The point is that in Ref. 26 they investigated a short sample, and such edge effects can be substantial (the initial distribution of the current density has quite strong irregularities so that the characteristic times of the redistribution of the magnetic field near the sample surface should be small).

It is difficult to solve this problem mathematically. We have therefore measured the growth rate of the transverse magnetic field for a rectangular tin sample. Our sample had the same dimensions as the samples of Ref. 26 ( $1 \times 1 \times 2$  cm) and a somewhat lower residual resistance (the time constant of the damping of the eddy currents was  $\sim 5$  sec). A miniature coil was used to measure the transverse magnetic field  $H$  in a region of  $\sim 2$  mm diameter located halfway between the equatorial line and the edge of the sample. The coil voltage, proportional to  $\partial H_1 / \partial t$ , reached a maximum approximately 30 msec after the solenoid current was turned off. The effect was observed also in the normal state ( $T > T_c$ ), and when the temperature was lowered below  $T_c$  the magnitude of the effect still increased, owing to the strong dependence of the resistance of the TM state on the current density. The quantitative results were the following: at  $H_0 = 4H_c = 520$  Oe ( $T = 2.7$  K) the value of  $H_1$  at the measurement point reached  $0.05H_c$  at approximately 40 msec after opening the solenoid supply circuit; at that instant of time  $\partial H_1 / \partial t = 300$  Oe/sec. These results depended little on the angle between  $H_0$  and the sample surface.

We note also that in the normal state, when the turned-off magnetic field  $H_0$  was increased, the transverse magnetic field increased quite faster than  $H_0$ . This is obviously due to the local overheating of those sections of the sample where the current density was a maximum. The overheating is accompanied by a decreased resistance and hence by an increased rate of equalization of the current density in the sample. Thermal effects undoubtedly play an essential role also in measurements below  $T_c$ . In the case of aluminum samples, whose thermal conductivity at the measurement temperature is smaller, the thermal effects should lead to an additional increase of the transverse magnetic

field.

Such a time dependence of  $H_1$  can explain fully the picture observed in Ref. 26 in the central part of the sample. The transverse magnetic field, which is present both above and below the equatorial line of the sample, leads to the onset of normal regions in the TM-state layer, with  $H_1$  having opposite signs on the two sides of the equatorial line and with both structures moving towards each other. In such a motion, annihilation of some of the normal regions is possible, while some of them can apparently reach the opposite edge of the sample.

<sup>1</sup>The measured current-voltage characteristics of these samples were published earlier.<sup>5</sup>

<sup>2</sup>It is seen from Fig. 13b that the period of the structure increases approximately like  $1/H_1$ , so that the dimensions of the normal regions remain practically unchanged with decreasing  $H_1$ , and we did not encounter a situation in which the resolving power of the microcontacts or of the measurement circuit would be insufficient.

<sup>1</sup>D. Shoenberg, Superconductivity, Cambridge, University Press, 1938, p. 59.

<sup>2</sup>I. L. Landau and Yu. V. Sharvin, Pis'ma Zh. Eksp. Teor. Fiz. **10**, 192 (1969) [JETP Lett. **10**, 121 (1969)].

<sup>3</sup>I. L. Landau and Yu. V. Sharvin, Pis'ma Zh. Eksp. Teor. Fiz. **15**, 88 (1972) [JETP Lett. **15**, 59 (1972)].

<sup>4</sup>I. L. Landau, Zh. Eksp. Teor. Fiz. **67**, 250 (1974) [Sov. Phys. JETP **40**, 126 (1974)].

<sup>5</sup>I. L. Landau, Pis'ma Zh. Eksp. Teor. Fiz. **23**, 516 (1976) [JETP Lett. **23**, 471 (1976)].

<sup>6</sup>V. T. Dolgoplov and S. I. Dorozhkin, Pis'ma Zh. Eksp. Teor. Fiz. **27**, 459 (1978) [JETP Lett. **27**, 430 (1978)].

<sup>7</sup>S. I. Dorozhkin and V. T. Dolgoplov, Solid State Commun. **30**, 205 (1979).

<sup>8</sup>V. T. Dolgoplov and S. S. Murzin, Zh. Eksp. Teor. Fiz. **76**, 1740 (1979) [Sov. Phys. JETP **49**, 885 (1979)].

<sup>9</sup>I. L. Landau, Zh. Eksp. Teor. Fiz. **76**, 1749 (1979) [Sov. Phys. JETP **49**, 889 (1979)].

<sup>10</sup>A. F. Andreev and P. Tekel', Zh. Eksp. Teor. Fiz. **62**, 1540 (1972) [Sov. Phys. JETP **35**, 807 (1972)].

<sup>11</sup>A. F. Andreev and W. Bestgen, Zh. Eksp. Teor. Fiz. **64**, 1865 (1979) [Sov. Phys. JETP **37**, 942 (1979)].

<sup>12</sup>W. Bestgen, Zh. Eksp. Teor. Fiz. **65**, 2097 (1973) [Sov. Phys. JETP **38**, 1048 (1974)].

<sup>13</sup>L. P. Gor'kov and O. N. Dorokhov, Zh. Eksp. Teor. Fiz. **67**, 1925 (1974) [Sov. Phys. JETP **40**, 956 (1974)].

<sup>14</sup>A. F. Andreev and Yu. K. Dzhikaev, Pis'ma Zh. Eksp. Teor. Fiz. **26**, 756 (1976) [JETP Lett. **26**, 590 (1976)].

<sup>15</sup>W. Bestgen, Zh. Eksp. Teor. Fiz. **76**, 566 (1979) [Sov. Phys. JETP **49**, 285 (1979)].

<sup>16</sup>I. L. Landau, Zh. Eksp. Teor. Fiz. **75**, 2295 (1978) [Sov. Phys. JETP **48**, 1158 (1978)].

<sup>17</sup>C. J. Gorter, Physica (Utrecht) **23**, 45 (1957).

<sup>18</sup>C. J. Gorter and M. L. Potters, Physica (Utrecht) **24**, 169 (1958).

<sup>19</sup>Yu. V. Sharvin, Pis'ma Zh. Eksp. Teor. Fiz. **2**, 287 (1965) [JETP Lett. **2**, 183 (1965)].

<sup>20</sup>Yu. V. Sharvin and I. L. Landau, Zh. Eksp. Teor. Fiz. **58**, 1943 (1970) [Sov. Phys. JETP **31**, 1047 (1970)].

<sup>21</sup>Yu. V. Sharvin, Zh. Eksp. Teor. Fiz. **48**, 984 (1965) [Sov. Phys. JETP **21**, 655 (1965)].

<sup>22</sup>Yu. V. Sharvin, Zh. Eksp. Teor. Fiz. **38**, 298 (1960) [Sov. Phys. JETP **11**, 216 (1960)].

<sup>23</sup>R. N. Goren and M. Tinkman, J. Low Temp. Phys. **5**, 465 (1971).

<sup>24</sup>A. F. Andreev, Zh. Eksp. Teor. Fiz. 51, 1510 (1966) [Sov. Phys. JETP 24, 1019 (1966)].  
<sup>25</sup>A. F. Andreev and Yu. V. Sharvin, Zh. Eksp. Teor. Fiz. 53, 1499 (1967) [Sov. Phys. JETP 26, 865 (1968)].

<sup>26</sup>S. I. Dorozhkin and V. T. Dolgoplov, Zh. Eksp. Teor. Fiz. 77, 2443 (1979) [Sov. Phys. JETP 50, 1180 (1979)].

Translated by J. G. Adashko

## Frequency-angle spectrum of light scattering by polaritons and interference of susceptibilities of different orders

O. A. Aktsipetrov, V. M. Ivanov, and A. N. Panin

Moscow State University

(Submitted 29 October 1979)

Zh. Eksp. Teor. Fiz. 78, 2309-2315 (June 1980)

We investigate the singularities of the frequency-angle spectra of spontaneous parametric scattering of light by polaritons in a number of ferroelectric crystals such as lithium niobate, potassium dihydrophosphate, lithium formiate, iodic acid, and others. It is shown that most of the observed singularities can be successfully explained within the framework of the model of interference between the background and resonant values of the first- second- and third-order susceptibilities of the medium.

PACS numbers: 77.80. - e, 78.20.Dj, 71.36. + c

The rapid advances in laser spectroscopy of media have led to the appearance of new types of spectroscopy, in which information is provided not only by the frequency  $\omega$  of the scattered or absorbed electromagnetic waves, but also by their wave vector  $\mathbf{k}$ . One can speak therefore of "two-dimensional" spectroscopy in  $(\omega - \mathbf{k})$  space. One of the phenomena on whose basis a method of spectroscopy in  $(\omega - \mathbf{k})$  space can already be developed to a sufficient degree is spontaneous parametric scattering of light by polaritons, LSP (see, e.g., Ref. 1). However, extensive applications of this method are impeded by the fact that the LSP has not been sufficiently well studied, particularly near the natural vibrations of the lattice.

We investigate in this paper the effect of the interference of the first-, second-, and third-order susceptibilities of the medium in the vicinity of an isolated lattice vibration [characterized by a dipole moment and a Raman-scattering (RS) tensor] on the frequency-angle distribution of the intensity of light scattering by polaritons. The singularities of the light scattering by polaritons in lithium niobate ( $\text{LiNbO}_3$ ), lithium iodate ( $\text{LiIO}_3$ ), potassium dihydrophosphate ( $\text{KH}_2\text{PO}_4$ ), deuterated potassium dihydrophosphate ( $\text{K}(\text{H}_x\text{D}_{1-x})_2\text{PO}_4$ ), ammonium dihydrophosphate ( $\text{NH}_3\text{H}_2\text{PO}_4$ ), lithium formiate and deuterated lithium formiate ( $\text{LiHCOO}\cdot\text{H}_2\text{O}$  and  $\text{LiHCOO}\cdot\text{D}_2\text{O}$ ), and iodic and deuterated iodic acids ( $\text{Li}_x\text{Na}_{1-x}\text{HCOO}\cdot\text{H}_2\text{O}$ ), ( $\alpha\text{-HIO}_3$ ,  $\alpha\text{-DIO}_3$ ) are explained within the framework of the interference of the background and resonant values of the susceptibilities.

The intensity of a signal wave with a frequency  $\omega_s$  and a wave vector  $\mathbf{k}_s$  in a three-frequency parametric process is determined by the imaginary part of the increment  $\Delta\varepsilon(\omega_s)$  added to the dielectric constant by the strong pump field ( $\omega_L$  and  $\mathbf{k}_L$ ). The signal wave has a maximum gain and consequently a maximum intensity if the condition of spatial synchronism

$$\mathbf{k} = \mathbf{k}_L - \mathbf{k}_s \quad (1)$$

is satisfied. Here  $\mathbf{k}$  is the wave vector of the additional (polariton) wave, whose frequency is determined by the condition

$$\omega = \omega_L - \omega_s. \quad (2)$$

The conditions (1) and (2) lead to a unique relation between the frequency-angle spectrum of the scattering, on the one hand, and the dispersion characteristics of the medium, on the other.

Knowledge of the dispersion of the medium in the transparency region, which usually contains the signal and pump frequencies, together with the LSP spectra, makes it possible to determine the dispersion of the medium at the polariton-wave frequency, which can land in the region of the natural vibrations of the lattice. In those cases when the polariton-wave frequency is far enough from the frequencies of the resonances (by several line widths), information on the scattering medium is provided by the following elements of the of the LSP spectra:

a) The tuning curve, determined from the condition

$$\left. \frac{\partial I(\omega_s)}{\partial k} \right|_{\omega = \text{const}} = 0,$$

yields information on the dispersion curve of the lattice and the function  $\varepsilon'(\omega)$ .

b) The angular and spectral widths of the tuning curve yield information on the absorption coefficient and the function  $\varepsilon''(\omega)$ .

c) The scattering intensity (integrated over the scattering angle at the given frequency, as well as the amplitude) yields information on the components of the quadratic-susceptibility tensor  $\chi_{ijk}$ .

On the other hand, if the polariton frequency approaches the lattice resonant frequency, the linear and